International Journal of Computational Intelligence and Applications
Vol. 20, No. 1 (2021) 2150005 (22 pages)

DOI: 10.1142/S146902682150005X

A Computer Vision-Based Method for Classification of Red Meat Quality After Nitrosamine Appendage

Monika Arora* and Parthasarathi Mangipudi†

Department of Electronics and Communication Engineering
Amity School of Engineering and Technology
Amity University Uttar Pradesh, Noida, India
**monika4dec@gmail.com*
†*psmangipudi@amity.edu*

Received 24 March 2020
Revised 24 July 2020
Accepted 27 July 2020
Published 22 January 2021

Nitrosamine is a carcinogenic chemical used as a preservative in red meat whose identification is an ordeal. This paper presents a computer vision-based non-destructive method for identifying quality disparities between preservative treated and untreated (control) red meat. To access the discrepancy in the quality of red meat, both traditional machine learning and deep learning-based methods have been used. Support vector machine (SVM) classifier and artificial neural network (ANN) models have been used to detect the presence of nitrosamine in test samples. The paper also made use of different pre-trained deep convolutional neural networks (DCNN) with transfer learning approach such as ResNet-34, ResNet-50, ResNet-101, VGG-16, VGG-19, AlexNet and MobileNetv2 to examine the presence of nitrosamine in the food samples. While the ANN classifier performed better in comparison to the SVM classifier, the highest testing accuracy and F1-score were obtained using the deep learning model, ResNet-101 with 95.45% and 96.54%, respectively. The experimental results demonstrate an improved performance in comparison to the existing methods; indicating the feasibility of the proposed work for food quality control in real-time applications.

Keywords: Deep convolutional neural network; transfer learning, image classification; network training; traditional machine learning.

1. Introduction

As a part of an overall salubrious diet, red meat (capra aegagrus hircus) which is widely consumed has rich amounts of vitamins, minerals, antioxidants and proteins that can have profound effects on human health.[1] Throughout the evolution of mankind, people have been eating red meat, however, the quality of meat consumed today is different from the meat which people used to consume in past.[2] One of the major causes for the depreciated quality of red meat is the addition of preservatives.[3] The color of fresh red meat is light red to brick red which fades to brown with time.[4] To prevent discoloring of meat, preservatives like nitrites (E-249 and E-250) and

*Corresponding author.

nitrates (E-251 and E-252) are added so that the shelf life of the food item is elongated.[5] Serious neurotoxin, nitrosamine is produced by nitrites and nitrates, which splits up into nitrosonium cation and water.[6] The redness of meat is nurtured by adding nitrosamine as a preservative, which is a proven threat to consumer's health.[7] Preservatives are chemicals that not only destroy its nutritious value but also promote the risk of cancer, heart disease and other promotional diabetes.[8] It is necessary to recognize and classify the toxic preservatives in food items before it is fed to the consumer. The traditional chemical laboratory-based technique is a validated approach used to diagnose the subsistence of nitrosamine preservatives in food items. Such chemical-based methods are slow, tedious and destroy the food sample with the use of expensive instruments.[9] To overcome these limitations, the design of a Computer Vision System (CVS) may be adopted that measures the discriminatory variations of spatial information in the visuals of food items. CVS is a cost-effective method of measurement as it supports re-utilization of samples, provides fast processing speed and does not require any provision of trained manpower. It is a viable tool for food quality assessment in real-time applications ensuring better human-health.[10] In recent years, researchers have filed patents in the field of quality assessment of food products wherein the edibility of food samples was examined using imaging method.[11]

Image processing techniques have been extensively explored for the classification and analysis of food quality in the research articles and patents. To this reference, broad review of hyperspectral imaging has been proposed for quality assessment of several vegetarian and non-vegetarian food products.[12,13] A supervisory information system was invented by a patent in Ref. 14 which employs a video camera device for image acquisition; an appropriate wavelet decomposition technique has been applied for analyzing the acquired image by removing unwanted noise wavelet coefficients so that the quality of meat products can be determined. The quality of the lamb meat was determined in terms of absorption spectra by designing a Multiple Regression Model (MRM) with a high correlation coefficient.[15] A prediction model for meat quality evaluation was designed by reducing the extracted features using Principal Component Analysis (PCA).[16] Discriminatory features have been analyzed and intramuscular meat fat tissue was quantified from its original microscopic images.[17] Support Vector Machine (SVM)-based classification of chopped apples has been obtained which identifies enzymatic browning.[18] Average spectra of the meat samples were obtained; multivariate analysis was extracted from the reduced set of features which were acquired by PCA.[19] Least Mean Square (LMS) value of weight and slaughter's age has been calculated that gives a high correlation coefficient determining the quality of the sample under test.[20] The freshness of meat samples was identified by calculating the Mean Square (MS) value followed by the application of Analysis of Variance (ANOVA) and F-test.[21] The statistical analysis of the meat samples was obtained by measuring the probability value which validated the investigation against the results of colorimetric test.[22] The spatial information has been obtained by perceptually applying the concept of Anti-Textons for the

classification and retrieval of food images.[23] The quality of grass carp fish fillet was evaluated by designing Least Squares-Support Vector Machine model (LS-SVM) for quantitative analysis of the image in order to select optimum wavelength using Successive Projections Algorithm (SPA).[24] Spectral and texture features were extracted from the hyperspectral images of chicken meat followed by the application of feature fusion technique such that optimum wavelength can be selected using SPA.[25] In traditional machine learning, classification accuracy depends on two factors, first, the strategy designed in the extraction of handcrafted features and second, passing of most discriminatory features over to the preceding algorithm, thereby causing an increase in the computational complexity and subsequently, decrease in the system accuracy. To overcome this challenge, end-to-end learning approach based on deep learning has been proposed, which can be extended to other food items.[26]

Lately, deep learning has been applied to different fields of image processing like medical imaging,[27,28] satellite imaging,[29] microscopic imaging,[30] agro-food imaging[31] and many more. Some of the recent state of the art on image classification using deep learning includes identification of objects using scratch training model, fine-tuning of model and augmentation of dataset.[32] Some of the research studies also emphasize on image processing techniques using deep convolutional neural networks (DCNN) based on the concept of transfer learning.[33] Although deep learning has several fascinating advantages like efficient handling and transferring of most robust and discriminatory features[31] for image analysis that provides an ascension to the performance measurement parameters such as accuracy while handling larger dataset when compared to traditional machine learning technique.[34]

Currently, researchers have also applied CNN methods in assessing the quality and safety of food products by analyzing its spectra[35] and RGB components.[36] CNN method may be acknowledged as a significant approach for automatic learning of deep features obtained from input digital information for subsequent classification and data mining tasks related to the food industry, since it can appropriately replace conventional evaluation techniques of food items like spectrophotometry, digital cameras, electronic nose, etc. However, CNN architecture also requires considerable hardware like Graphics processing unit (GPU) to run effectively and efficiently on larger datasets such as ImageNet dataset which consists of 3.2 million images. ImageNet dataset exhibits enough categorization of sample images and instances identified using CNN model wherein acute overfitting or underfitting had been avoided.[37]

From the state of art, the following keynotes were observed:

- Although various sets of statistical and texture features have been extracted through traditional machine learning methodology, still nitrosamine identification in food items has not been directly accounted.
- However, more advanced deep learning methods have been designed in recent times but the harmful preservative identification in food items like red meat has not been explored exhaustively.

Hence, the proposed research work aims to design a non-destructive computer vision-based classification method for the identification of nitrosamine preservative in red meat samples using a traditional machine learning-based model and pre-trained deep convolutional neural networks via transfer learning approach.

The application of deep learning is shown to be useful in conducting a random investigation of red meat samples from a whole lot of samples in order to assess the quality and safety of food items.

The most pertaining research work in the area of red meat quality assessment using different computer vision techniques has been shown in Table 1.

Several design challenges have been addressed in the proposed research work. Computer vision-based classification of red meat samples may be validated against

Table 1. Comparative table between few existing methods.

Reference	Sample Size	Algorithm Used	Result Analysis
15	126 lamb meat samples Training dataset: 84 and testing dataset: 42	• Hierarchical variable selection method (UVE–SPA–CSA) • Uninformative variable elimination (UVE) • Successive projections algorithm (SPA) • Clonal selection algorithm (CSA)	• Correlation coefficient of input images: 0.95, 0.80 and 0.91 • Prediction to deviation (RPD) ratio: 4.13, 1.31 and 2.53.
16	74 beef meat samples Training dataset: 60 Testing dataset:14	• Normalized Radial Basis Function (RBF) neural network, • Bayesian Ying-Yang Expectation Maximization algorithm • Fuzzy principal component algorithm	• Classification accuracy:92.86 %. • Overestimate prediction: 22.76%
19	420 samples of chicken, pork and beef meat, adulterated with: Pork- 210 Beef- 210	• Root mean square error of calibration (RMSEC) • Root mean square of cross-validation (RMSECV) • Root mean square of prediction (RMSEP) • Coefficient of determination of calibration, cross-validation, and prediction • RDP.	• Coefficient of prediction: 0.83 and 0.94 • RDP: 1.96 and 3.56 • Ratio of error range (RER): 10 and 18.1.
20	180 bull breeds of lean cattle samples. 60 samples each of 3 breeds.	• Analysis of variance (ANOVA) technique • Measurement of factor mean square • Comparison with F-test at 95% confidence interval.	• Correlation coefficient: 0.40 and 0.26 at 95% confidence interval.
22	45 samples Beef: 15 Pork: 15 Chicken: 15	• Image analysis using photoshop • Chi square test, T-test • Spearman rank correlation test	• Strategic significance of CVS (p-value < 0.05 -0.0001).

Table 1. (*Continued*)

Reference	Sample Size	Algorithm Used	Result Analysis
55	72 pork meat samples. Training dataset: 48 Testing dataset: 24	• Adaboost algorithm • BPANN learning algorithm	• Correlation coefficient: 0.932 • RPD:2.885.
56	210 pork meat samples. Training dataset: 140 and testing dataset: 70	• Feature level fusion OF texture feature • PLS Regression • SPA	• Correlation coefficient: 0.898, 0.876 and 0.924
57	75 meat samples, each of lamb, beef, pork and fat Training dataset: 57 Testing dataset: 18	• SVM classifier • Convolutional neural network (CNN) model	• CNN model accuracy: 94.4%
58	1400 boneless pork loins. Training dataset: 1120 Testing dataset: 280	• 10-fold cross validation technique • RBF algorithm • SVM classification	• Prediction accuracy: 92.5% • Marbling score: 75%
35	75 meat samples of lamb, beef, pork and fat. Training dataset: 57 Testing dataset: 18	• Gray level co-occurrence matrix (GLCM) feature extraction • PCA • Design of CNN model from scratch	• Classification accuracy: 94%.
59	97,200-pixel spectra from 120 shrimp samples. Training dataset: 77,760 pixels. Validation dataset:19,440 pixels.	• Stacked auto-encoders (SAE) • Successive projections algorithm (SPA)	• Correlation coefficient: 0.921

the traditional laboratory technique to ensure the accuracy in context to food samples quality.

The main contribution of this paper is to design a framework for distinguishing treated from control red meat samples using traditional machine learning and deep learning-based methods. A descriptive analysis of the discriminatory statistical and texture features obtained from the segmented image have been considered useful in designing a dynamic application in the context to proposed traditional machine learning models. Feature selection and data reduction technique has been applied using different methods on the extracted features. Another contribution is the tuning of hyperparameters of pre-trained DCNN model by selecting optimum learning rate, the number of epochs and batch size to avoid over-fitting in order to obtain true classification error. The third contribution of the paper is to replace the last three layers of the pre-trained model and to compute the performance parameters of different pre-trained DCNN models. Last, all the proposed models trained on vast datasets could have a significant impact in the food industry for assessing the quality and safety of the food items in real-time applications ensuring better human health.

2. Materials and Methods

The following section presents the techniques involved in the qualitative assessment of red meat using conventional laboratory techniques.

2.1. *Red meat sample preparation and data collection*

The whole muscle from loin portion of the goat (breed: barbari) was purchased from Randhawa Poultry farm, Kapaskheda, Gurgaon, India. The red meat parts used for testing were the neck, leg, shoulder, ribs, loin, liver and kidney. Meat samples of size 5 cm × 5 cm × 5 cm were stored at a room temperature of 25°C for analysis. All the samples were labeled as control/treated samples.

2.2. *Laboratory testing for chemical analysis*

The control and treated samples were stored at a temperature of 2°C for simulation purposes having pH value of 5.4. American Chemical Society (ACS) grade sodium chloride and sodium nitrite used for solution preparation were procured from HiMedia labs, India. To study the nitrosamine presence, sodium chloride brine solution (NaCl 20 g/L) was used as blank, and sodium nitrite wet curing solution (NaCl 20 g/L, and $NaNO_2$ 150 mg/L) was used as treatment. For incubation of samples, Nisco manufactured Bio-Oxygen Demand (BOD) incubator has been used. Meat samples were immersed in solutions for 96 h in BOD incubator at a temperature of 8°C in a closed glass container. The operation range of this incubator is 5°C to 60°C, 220 Volts. Samples were taken out randomly from both solutions at a specific time interval (24, 48, 72 and 96 hours) and washed with distilled water. For conversion of sodium nitrite into nitrosamine, washed samples were cooked at a temperature of 120°C for 6 min under pressure to achieve full cooking with 100 ml water. The samples were taken out of the pressure cooker for further analysis after cooling them at room temperature. All the procedures were performed in duplicates. Sodium nitrite added with salt paced at an optimum temperature for cooking generates preservative which protects treated meat samples from microbial poisoning. This process forms nitric oxide which reacts with muscle myoglobin and form nitric oxide metmyoglobin. This nitric oxide metmyoglobin was responsible for pre-cook brown pigment in treated meat. During cooking, nitrosylhemochromogen (NHC) was formed from nitric oxide metmyoglobin due to the denaturation of the protein part of myoglobin.

2.3. *Validation of nitrosamine in red meat using conventional method*

The identification of nitrosamine produced in the samples was validated by the method described by Ref. 38 using Griess reagent with slight modifications. The test was conducted by mixing 1 ml of Griess reagent and 1 ml of hydrochloric acid with 2 gm of finely ground meat sample in a test-tube. The mixture is heated at a temperature of 40°C for 30 min. All the treated samples showed red-violet color

confirming the presence of nitrosamine in them, unlike control samples. Alkalinity and pH were not monitored as process optimization was not the focus of the present work. The chemical parameters were ignored while identifying nitrosamine in the red meat samples as they were used for quantification of this toxic substance. The proposed research work produces a binary classification of the test samples indicating only the presence or absence of nitrosamine in the red meat sample.

2.4. *Storage technique of meat samples*

In this paper, 62 pre-processed meat samples were analyzed for their freshness identification. 24 samples were control samples that were not exposed to nitrosamine chemical and 38 samples were treated with the chemical. Treated and control red meat samples were placed in a beaker containing nitrosamine chemical and the aqueous solution respectively at room temperature of 25°C as shown in Fig. 1.

All control samples were stored for 96 h in a frost-free refrigerator (Samsung T28K3723UT/NL/2016) whereas the pattern of storage of treated samples was different from former. The treated samples were exposed to chemical for a period of hours. The concentration of nitrosamine develops in sample based on their storage pattern. After the exposure of chemical, these treated samples were stored in a refrigerator maintained at a temperature of 3°C.

2.5. *Development of image acquisition system*

For acquiring images of meat samples, a hardware setup can be designed which may comprise of various combinations of Compact Fluorescent Lamps (CFL) tube lights like set of four CFL and three tube lights for illumination assembled with a camera placing position. CFL lamp (Osram DULUXSTAR) operates at a power rating of 35 W, a color temperature of 6500 K, 220-240 V voltage of alternating current with a frequency of 50 Hz and 2100 lumens. Osram tube light (T5 RADIANCE G2 WT 14) has been employed in the image acquisition set up operating at a voltage of 230 V,

Fig. 1. Immersion of treated and control samples in a beaker.

50 Hz frequency. A digital Canon camera (IXUS 285 HS) has been used for the acquisition of image with a spatial resolution of 5184 × 3888 pixels with a horizontal and vertical resolution of 180 dpi having bit depth 24, the focal ratio of the camera was f/3.6 with 1/320 sec of exposure time, 4 mm of focal length and a maximum aperture of 3.6875 of camera optical lens. The next section presents the novel methodology designed for the identification of nitrosamine in the collected meat samples with the help of the designed image acquisition system.

3. Proposed Model

The proposed research work identifies the presence of nitrosamine in red meat samples by using traditional machine learning-based models and deep learning networks. While the classification techniques employed using traditional machine learning are based on the SV method and ANN) model, the technique using deep learning methods employs pre-trained networks of Deep Convolutional Neural Network (DCNN) models via transfer learning approach. This section gives a detailed overview of all the three techniques involved in the identification of the preservative in the food sample. Figure 2 shows the block diagram of the proposed methodology.

3.1. *Traditional machine learning methods for the detection of nitrosamine in food samples*

The newly synthesized compound, NHC formed in the meat sample is responsible for introducing biological change due to which color of the sample varies to bright pink or red color. The discrepancy in the color and physical properties of the meat sample leads to the variation of image pixels and its periodicity in spatial domain.

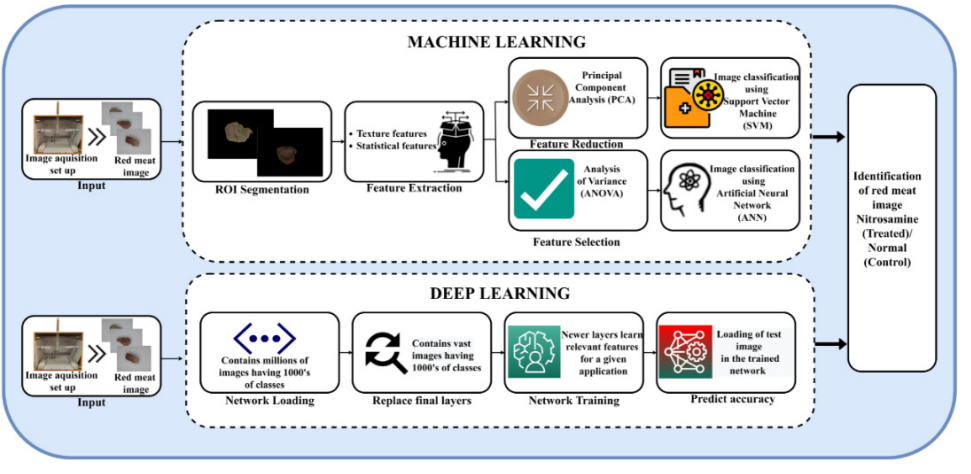

Fig. 2. Block diagram of proposed methodology.

The dissimilarity discriminates statistical and texture parameters of treated meat samples from control meat samples. In this paper, the images of meat samples were acquired using a digital camera. The captured images were used for feature extraction using the image processing technique. The acquired images of the meat samples undergo image pre-processing in order to pace down all the images to one standard level since each acquired image exhibits different property and characteristics from other captured images. Subsequently, the image segmentation step was applied on the pre-processed image to segment the region carrying maximum information.

3.1.1. *Region of interest (ROI) segmentation*

Red meat images were in RGB format having a size of 820×581 pixels. Input images carries red meat portion with background region. Pixels associated with red meat region carries meaningful information. The value of pixels of red meat portion varies discriminately with storage period, so this region is taken as ROI. RGB sample images were paced down to a perceptual uniformity by converting into Lab color space model. Conversion established compatibility with the segmentation process and the illumination condition within which the sample images have been captured. In this paper, the K-means clustering algorithm has been adopted for segmentation of ROI as it is one of the most popular methods suitable for splitting the image into clusters of similar information.[39] It is obtained by minimizing the squared error function as shown in Eq. (1) which partitions d, number of data points into c, number of clusters and computes Euclidian's distance between a_n, data points and b_m, centroid for cluster m.

$$S(E) = \sum_{m=1}^{c} \sum_{n=1}^{d} (\|a_n - b_m\|)^2. \tag{1}$$

Three distinct clusters of disparate information have been obtained as shown in Fig. 3.

The addition of two clusters (Clusters 2 and 3) provides segmented ROI in RGB format. Figure 4 shows the method used for the segmentation of red meat pixels.

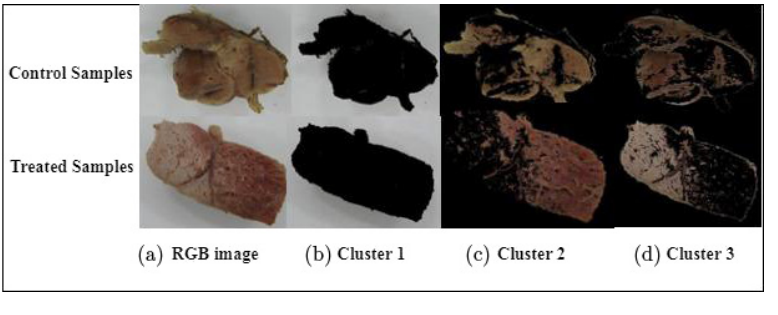

Fig. 3. Control and treated cluster images (a) RGB image, (b) Cluster 1, (c) Cluster 2 and (d) Cluster 3.

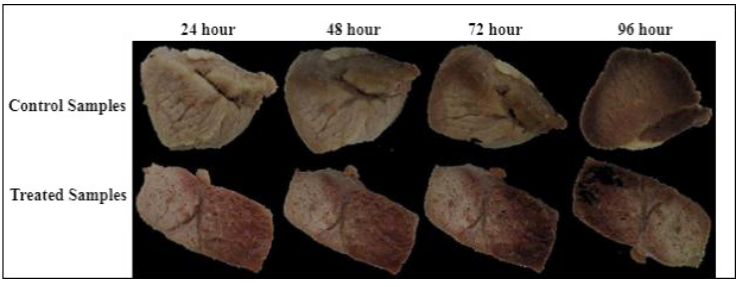

Fig. 4. Segmentation of ROI images of control samples.

3.1.2. *Feature extraction from segmented ROI*

The resultant image was converted into grayscale and 18 statistical and texture features have been extracted and further analyzed. Pixel information has been obtained by measuring features like the first order, second order and higher order. First-order statistical features provide information related to individual pixel value rather than neighboring pixels. The extracted features which measure the variability of Pixel Intensity (PI) of an image in the spatial domain are mean, standard deviation and variance. The mean (μ) of an image refers to the average value of the PI. Standard deviation (SD) refers to the variation of PI from its mean value. Variance (V) is the mean squared deviation from the mean value of its PI. Gray level co-occurrence matrix (GLCM) features were also extracted from the image as they consider the spatial relation of pixels in the region. The extracted GLCM features are contrast, energy, correlation and homogeneity. Contrast (C) of the image is defined as the difference between the maximum and minimum PI. Energy (E) depicts the uniformity in the image by measuring the recurrent pair of PI. Correlation (C_r) is defined as how a pixel is correlated to its neighboring pixel over a complete image. Homogeneity (H) depicts the homogenous values of pixels in low and high contrast images. As part of experiments, higher-order Gray level Run Length Matrix (GLRLM) features were also extracted as they provide valuable textural information of the region.[40] The extracted features were Short Run Emphasis (SRE), Long Run Emphasis (LRE), Gray-Level Non-uniformity (GLN), Run Length Non-uniformity (RLN) and Run Percentage (RP) respectively. Later, two additional features, namely Low Gray-Level Run Emphasis (LGRE) and High Gray-Level Run Emphasis (HGRE) proposed by Ref. 41 were also used for analysis. Also, four more features depicted by Ref. 42 like Short Run Low Gray-Level Emphasis (SRLGE), Short Run High Gray-Level Emphasis (SRHGE), Long Run Low Gray-Level Emphasis (LRLGE) and Long Run High Gray-Level Emphasis (LRHGE) were also obtained for analysis of identification of nitrosamine in the control and treated red meat samples.

3.1.3. *Classification of red meat sample using LOOCV-based SVM technique*

Feature reduction was used to reduce the number of features to be fed into the SVM classifier. Principal Component Analysis (PCA) was used to remove redundant features. Principal Components carries the most discriminatory information. Principal components having the highest variance were selected while the ones with smaller variance were rejected. In the proposed method, two principal components were chosen. In other words, the feature space was then a two-dimensional space and where a line needed to be drawn so that the two classes could be separated via an SVM classifier. Figure 5 shows the two principal components of the control and treated samples.

The image dataset was split into two parts, i.e., training and testing dataset for classification. Leave-One-Out-Cross-Validation (LOOCV)-based SVM technique was used for the identification of toxic preservative in red meat. Keeping in mind a smaller dataset at hand, LOOCV was preferred. Each observation was used as a test sample while the rest of the data points were used to train the classifier. This step was repeated for all the samples. Hyperplane was obtained from various data points of the training dataset.[43] Figure 6 shows the output of the SVM classifier.

3.1.4. *Classification of red meat sample using ANN model*

The cost of handling a large set of features could be reduced by feature selection. Using a statistical technique, Analysis of Variance (ANOVA), only the statistically significant features could be retained out of the total feature set.[44,45] In this method, ANOVA is used for testing the significance of the features extracted from segmented ROI. In this paper, one-way ANOVA test is employed, which refers to one independent variable, i.e. the extracted feature and two output levels, i.e. healthy or unhealthiness of the red meat sample. A confidence level of 95% is used here, so the significance level, $\alpha = 0.05$. This test is performed on all the 18 extracted features

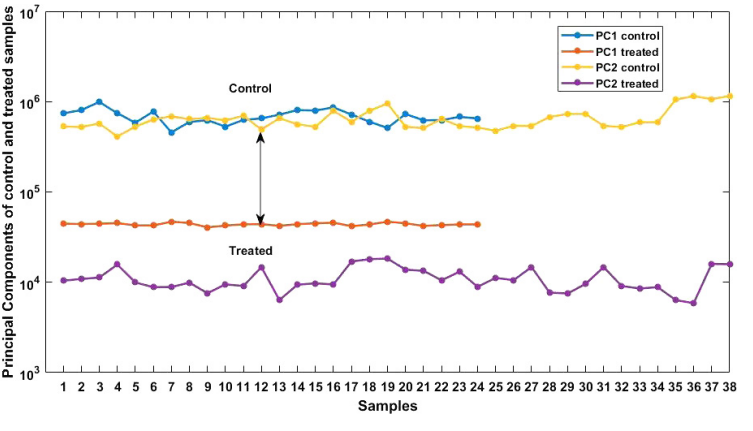

Fig. 5. Principal components of control and treated samples.

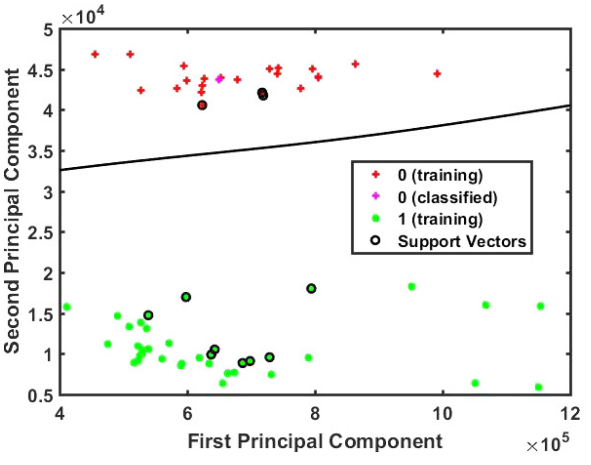

Fig. 6. LOOCV-based SVM response of principal components of control and treated samples.

individually and it provides a p-value for each feature. This value indicates the significance of a feature in determining the quality assessment of red meat.

Table 2 shows the p-values of all the extracted features with a clear identification of 7 features which are deemed to be statistically significant out of the 18 features which were extracted in the pre-processing step.

Most significant features were used as the inputs to the ANN network and the output of the binary classifier predicts the quality of red meat samples whether healthy (control) or unhealthy (treated). In the proposed work, a feed-forward neural

Table 2. P-values of extracted features.

Feature	Treated	Control	Significance Level $\alpha = 0.05$
E	0.0025	0.00000002	P-value $< \alpha$ Most significant
μ	0.0027	0.0004872	
SRE	0.0033	0.0000074	
C	0.0047	0.000000012	
V	0.006	0.00045738	
SD	0.0061	0.0004597	
SRLGE	0.0375	0.0014	
LGRE	0.1118	0.2168	P-value $> \alpha$ Least Significant
SRHGE	0.1186	0.7281	
HGRE	0.1459	0.844	
RP	0.1591	0.9532	
LRHGE	0.2438	0.9616	
GLN	0.2511	0.7758	
LRLGE	0.3436	0.7111	
RLN	0.3664	0.7743	
LRE	0.6059	0.1164	
H	0.8432	0.11	
C_r	0.8589	0.223	

network has been implemented for the qualitative analysis of red meat samples. To achieve minimum localization error in the training network, Levenberg–Marquardt (LM) training algorithm has been selected. Also, this algorithm exhibits better speed and efficiency in comparison to other algorithms.[46] In this experimental research work, the designed ANN architecture consists of seven inputs, 25 hidden neurons in the hidden layer and one output layer as shown in Fig. 7. The number of hidden layers and hidden neurons has been carefully selected in order to avoid overfitting. For validation and testing purposes, the set of 62 samples were randomly divided into 70% (44 samples) for training purposes, 15% (9 samples) for validation and 15% (9 samples) for testing purposes.

3.2. *Classification of red meat sample using deep convolutional neural networks (DCNN)*

DCNN normally require a large dataset in order to achieve high classification accuracy. Though, in various disciplines, the procurement of such a larger database is challenging. In such problematic situations, the utilization of entrenched DCNN models like ResNet-34,[47] ResNet-50,[47] ResNet-101,[47] VGG-16,[48] VGG-19,[48] Alexnet,[33–49] MobileNetv2[50] pretrained on larger database (ImageNet) have evidenced to be a substantial boon for comprehending multi-discipline image classification crunch via transfer learning approach.[51] The various layers of DCNN models extract several levels of information from the red meat image dataset. The filters related to the preliminary layers extract the low-level image information associated like the edge and the color of the input image whereas the filters at the latter layers gives the abstractions existing in the image like texture and shape. In the proposed research work, the transfer learning approach has been incorporated because of its twofold qualities, first; it is cheap to use and second; it can effectively classify smaller image dataset by transferring the knowledge learned from the DCNN model trained on a larger dataset in comparison to training a DCNN model from scratch.[52] With the fine-tuning of hyperparameters, the pre-trained DCNN model has outpaced DCNN model designed from scratch in various image processing applications.[51–53]

The structure of a typical DCNN comprises of a couple of convolution layers, pooling layers which are connected to fully connected layers. The convolutional

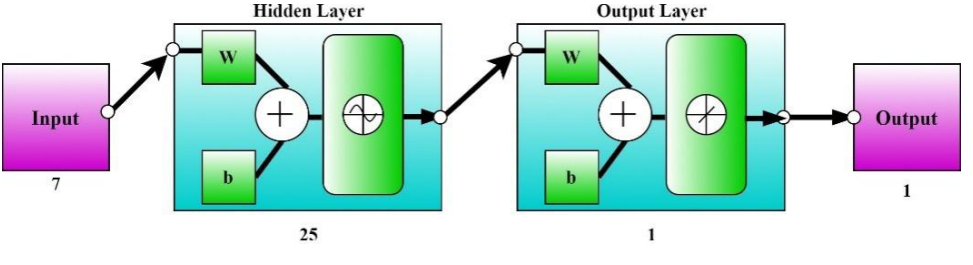

Fig. 7. Block diagram of neural network model.

layers behave like a feature extractor that is applied to the input image such that a feature map is created wherein the first layer extracts low-level features, subsequently, with the added layers high-level features are extracted from the red meat image. The objective of the pooling layer is to execute down sampling such that the dimensions of the extracted features could be reduced, and the most meaningful information associated with the meat image classification could be retained. Also, the spatial size of the convolved feature has been reduced which reduces the computational complexity of the problem.

The last layer is the fully connected (dense) layer which takes the outputs of convolution and pooling layers to classify the image dataset. The fully connected layer flattens the output obtained from preceding layers by converting it into a single vector and based on extracted feature assessment; weights are applied to predict the label using the softmax activation function. The fully connected output layer finally predicts the type of image whether control (non-nitrosamine) or treated (nitrosamine) red meat sample. Figure 8 shows the methodology adopted in the proposed research work.

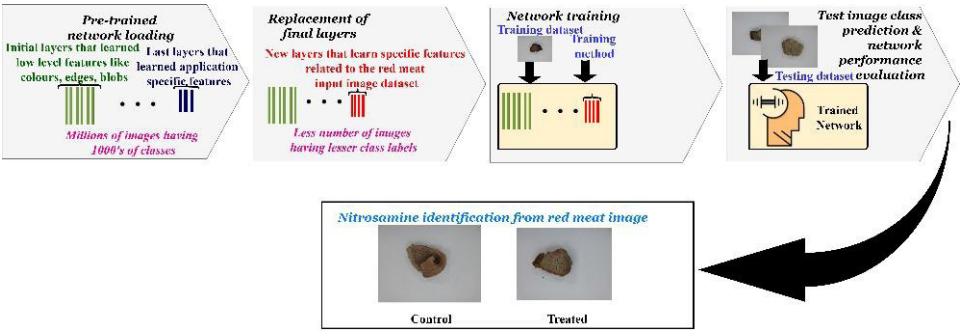

Fig. 8. Classification using pre-trained DCNN models via transfer learning approach.

Fig. 9. Data augmentation of meat image sample.

The unbalanced image dataset has been replicated to 129 images in order to analyze the image using DCNN pre-trained architecture. The replicated dataset was partitioned into a training dataset (85%) and the testing dataset (15%). The training dataset comprises of total 110 images wherein 68 images endure in the treated class and 42 images in control class; and testing dataset consists of 19 images. 20% of the training dataset (22 images) has been used as a validation dataset.

The proposed framework for executing deep learning models was implemented in the google collab environment with Python 3.6 as runtime type and GPU for accelerating the hardware. The pre-processing steps in DCNN include fine-tuning of hyperparameters like adjusting of batch size to 32 and handling of input images by using data bunch. Fastai libraries like fastai vision and fastai metrics were imported from fastai environment in order to retrieve as well as analyze the images of the dataset.[54] Data augmentation resulted in an increase in the size of the dataset by a factor of 8. The total set of images appended into the dataset were 880 images from (110 training images) $\times$ (2 flipping) $\times$ (1 maximum rotation) $\times$ (1 maximum zooming) $\times$ (2 random lighting) $\times$ (2 warping). Figure 9 shows various images as a result of data augmentation. After, augmentation, the dimensions of all the images were resized to 224×224 pixels in order to make them compatible with the initial layers of the pre-trained model.

4. Performances Measures

Different performance measures have been selected to test the efficiency of the proposed methodology. The classification accuracy of the model is related to sensitivity (or recall) and specificity represented in terms of true negative (TP), true positive (TP), false negative (FN), false positive (FP) as shown in Eqs. (2)–(4). TP refers to the number of treated meat samples labeled as nitrosamine meat, TN refers to the number of control meat samples labeled as non-nitrosamine meat, FP refers to the number of control meat samples labeled as nitrosamine meat and FN refers to the number of treated meat samples labeled as non-nitrosamine meat.

$$\text{Sensitivity} = \frac{\text{TP}}{\text{TP} + \text{FN}}, \tag{2}$$

$$\text{Specificity} = \frac{\text{TN}}{\text{TN} + \text{FP}}, \tag{3}$$

$$\text{Accuracy} = \frac{\text{TN} + \text{TP}}{\text{TN} + \text{TP} + \text{FN} + \text{FP}}. \tag{4}$$

The harmonic mean of sensitivity and precision is measured in terms of F1-score as shown in the following equation:

$$F1 - \text{score} = \frac{2 * \text{Recall} * \text{Precision}}{\text{Recall} + \text{Precision}}. \tag{5}$$

Table 3. Comparison of performance metrics of traditional machine learning and DCNN architectures.

Proposed Models		Classification Accuracy (%)	Specificity (%)	Sensitivity (%)	Precision (%)	F1-Score
Traditional machine learning models	LOOCV based SVM	98.38	100	50	**100**	66.66
	ANN	88.88	100	85.71	**100**	92.30
Pre-trained DCNN models	ResNet-34	86.36	100	78.57	**100**	87.99
	ResNet50	86.36	87.5	85.71	92.30	88.88
	ResNet-101	95.45	87.5	**100**	93.33	96.54
	VGG-16	59.09	25	78.57	64.70	70.96
	VGG-19	63.63	50	71.42	71.42	71.42
	Alexnet	90.90	100	85.71	100	92.30
	MobileNetv2	90.90	87.5	92.85	92.85	92.85

5. Results

The algorithms have been designed in MATLAB 2017a software on a processor Intel®, Core™, i3-5005U, CPU@2.00GHz, 4.00GB RAM, 64-bit operating system. The results of both the traditional machine learning models and the more recent deep learning models were noted and compared.

The classification results of the proposed models have been tabulated in Table 3. LOOCV-based SVM classifier gave a good classification accuracy of 98.38% but the sensitivity was surprisingly very low. It means that the number of false negatives is high. Because of which F1-score has suffered. ANN model has performed better in comparison to the SVM classifier. The recall value has increased and therefore F1-score has clearly increased. Experiments were done on various pre-trained deep learning models to evaluate their performance. Also, different DCNN models were used for experiments. VGG models did not fare well compared to other deep learning models. While AlexNet and MobileNetv2 models have performed significantly better, ResNet-101 model has given the best results with a classification accuracy of 95.45% and an F1-score of 96.54%.

6. Discussion

Tuning of hyperparameters like learning rate, selection of the optimizer and proper choice of the loss function is essential for the improved performance of the deep learning models. Experiments have been conducted to finetune the hyperparameters and to make the right choices for optimizer and loss function.

6.1. *Choice of learning rate*

The comparative pre-trained model accuracy has been computed for different learning rates. Table 4 shows the comparative accuracy where bold signifies the best value of accuracy for the corresponding learning rate.

Table 4. Comparative accuracy of pre-trained model with different learning rates.

Learning Rate	ResNet-34	ResNet-50	ResNet-101	VGG-16	VGG-19	Alexnet	MobileNetv2
10^{-2}	71.42	68.18	60.00	30.15	**63.63**	63.63	72.00
10^{-3}	72.63	70.13	90.90	47.62	**63.63**	86.36	80.36
10^{-4}	76.11	72.72	**95.45**	52.15	60.01	**89.47**	89.47
10^{-5}	**86.36**	**87.21**	86.36	**57.89**	61.11	**89.47**	**89.72**

Figure 10 represents the learning rate versus loss plot of ResNet-101 pre-trained model. The model gives the highest accuracy when trained with a learning rate of 10^{-4}.

6.2. *Effect of optimization technique*

The strategies involved in designing an optimization algorithm help to minimize the error function, $E(x)$, that depends on the trainable parameters which measure target values (control or treated) from the red meat image dataset. Weights (W) and bias (B) values of the network were the internal trainable parameters which were trained, optimized and updated. The method involved in the training not only measures the output values but also reduces the loss function of the model. The reduction of the loss directly improves the accuracy and efficiency of the model. In the proposed research work, the optimizer used for computation of adaptive learning rate of all trainable parameters and exponentially decaying of past gradients, was achieved by Adaptive Moment Estimation (Adam) method. The technique used by Adam optimizer endowed a computational fast designed model. Moreover, the estimates of the first and second moments of the gradients used in the proposed optimizer were

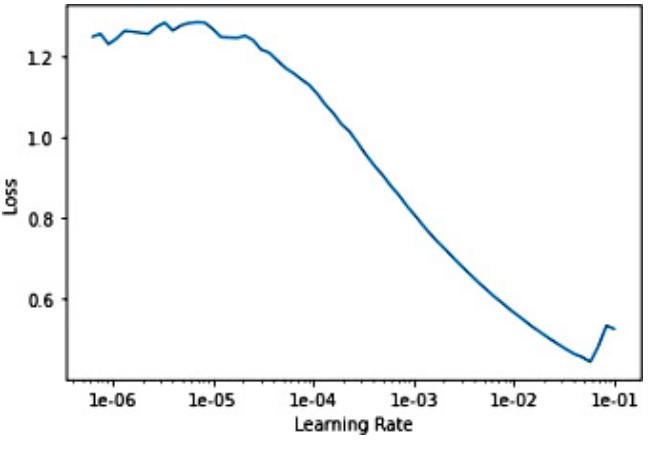

Fig. 10. Learning rate versus loss plot of pre-trained ResNet-101 network.

computed as follows, respectively.

$$\hat{m}_t = \frac{n_t}{1 - \beta_1^t}, \tag{6}$$

$$\hat{v}_t = \frac{v_t}{1 - \beta_2^t}. \tag{7}$$

Here, $\hat{m}_t$ is the value of mean which is the first moment, $\hat{v}_t$ is the second moment, i.e. variance, β_1 is 0.9 and β_2 is 0.99.

The final updation in the parameter was achieved as follows:

$$p_{t+1} = p_t - \frac{l_r}{\sqrt{\hat{v}_t} + \epsilon} * \hat{m}_t. \tag{8}$$

Here, p is the parameter with step size, t and l_r is the learning rate. The value of ϵ is 10^{-8}.

The learning speed of the proposed model was considerably improved which proves the efficiency of the selected optimizer. Moreover, the problems associated with vanishing learning rate was resolved by amending, first, parametric high variance and second, fluctuating loss function. Such a remarkable contribution of the proposed optimization technique makes it more superior to the other optimization algorithms.

6.3. *Effect of error and loss function*

The error refers to the difference between the true output (p) and the predicted output ($\hat{p}$). The function that measures this error is called the error function, $E(x)$ as shown in Eq. (9).

$$E(x) = p - \hat{p}. \tag{9}$$

In the proposed research work, the process involved in control and treated meat samples identification entails the usage of cross-entropy loss function, which is best suitable for dual-class labels as shown in Table 5. Gradients were the partial derivatives of the loss function calculated using optimization function continuously updates weights in order to minimize the loss function. In this paper, the flattened loss was used since it can flatten the output obtained from the previous layer to the next layer in one dimension.

The optimized and updated parameters obtained during model training through pre-trained network exhibits trainable parameters whereas the parameters that are neither optimized nor updated are usually computed in batch norm layer are

Table 5. Optimizer of proposed pre-trained networks.

Betas	Optimizer	Loss	Loss Function
(0.9, 0.99)	Adam	Flattened Loss	Cross entropy loss

non-trainable parameters. The input layer does not have to learn anything, so it has no linkage with any parameter. Max pooling layer reduces the dimensions of the image, so the trainable parameters were certainly not associated with this layer. The effective learning of the model will lead to accurate results only if appropriate optimization algorithms with suitable strategies were applied to the internal parameters of the model. The pre-trained ResNet-101 model achieved high accuracy because of two-fold reasons, first, the computed parameters attained an optimum value, second, the optimized value eventually paced up the learning process.

7. Conclusion

Nitrosamine is a carcinogenic preservative commonly added in red meat whose identification based on an analytical method has been an ordeal. In this paper, a novel computer vision-based method has been proposed for the qualitative detection of nitrosamine in red meat. Strategical framework was designed for observing the edibility of red meat by applying traditional machine learning methods as well as deep learning methods. In traditional machine learning methods, hand-crafted features were fed to the SVM classifier and ANN classifier respectively, while in the deep learning method, pre-trained DCNN models like ResNet-34, ResNet-50, ResNet-101, VGG-16, VGG-19, AlexNet and MobileNetv2 have been used via transfer learning approach. Evaluation measures for each of the proposed models were computed and compared. While the ANN model fared better than the SVM classifier in terms of F1-score, the deep learning-based pre-trained ResNet-101 model with transfer learning technique showed the highest accuracy of 95.45%. and an F1-score of 96.54%. In this paper, a significant novel contribution towards the identification of nitrosamine content in the red meat has been reported where ResNet-101 deep learning model has delivered more efficient and robust results than other deep learning and traditional machine learning models. This work attempts to initiate new aspects of research in the field of food quality assessment.

References

1. P. Williams, Nutritional composition of red meat, *Nutrition Dietetics* **64** (2007) S113–S119.
2. S. Ivanović, I. Pavlović and B. Pisinov, The quality of goat meat and it's impact on human health, *Biotechnol Animal Husbandry* **32**(2) (2016) 111–122.
3. R. Micha, G. Michas, M. Lajous and D. Mozaffarian, Processing of meats and cardiovascular risk: Time to focus on preservatives, *BMC Med.* **11**(1) (2013) 136.
4. T. T. Mensinga, G. J. Speijers and J. Meulenbelt, Health implications of exposure to environmental nitrogenous compounds, *Toxicol. Rev.* **22**(1) (2003) 41–51.
5. S. S. Herrmann, L. Duedahl-Olesen and K. Granby, Occurrence of volatile and non-volatile N-nitrosamines in processed meat products and the role of heat treatment, *Food Control* **48** (2015) 163–169.
6. L. M. Nollet and F. Toldrá (eds.), *Handbook of Processed Meats and Poultry Analysis* (CRC Press, 2008).

7. B. S. Furniss, *Vogel's Textbook of Practical Organic Chemistry* (Pearson Education India, 1989).
8. M. Gibis, Heterocyclic aromatic amines in cooked meat products: Causes, formation, occurrence, and risk assessment, *Comprehensive Rev. Food Sci. Food Safety* **15**(2) (2016) 269–302.
9. Y. Liu, B. G. Lyon, W. R. Windham, C. E. Realini, T. D. D. Pringle and S. Duckett, Prediction of color, texture, and sensory characteristics of beef steaks by visible and near infrared reflectance spectroscopy: A feasibility study, *Meat Sci.* **65**(3) (2003) 1107–1115.
10. P. McAllister, H. Zheng, R. Bond and A. Moorhead, Combining deep residual neural network features with supervised traditional machine learning algorithms to classify diverse food image datasets, *Comput. Biol. Med.* **95** (2018) 217–233.
11. R. A. Connor, U.S. Patent No. 10,458,845 (2019) Washington, DC: U.S. Patent and Trademark Office.
12. Z. Xiong, D. W. Sun, X. A. Zeng and A. Xie, Recent developments of hyperspectral imaging systems and their applications in detecting quality attributes of red meats: A review, *J. Food Eng.* **132** (2014) 1–13.
13. A. Bhargava and A. Bansal, Fruits and vegetables quality evaluation using computer vision: A review, *J. King Saud Univ.-Comput. Inform. Sci.* (2018).
14. X. Jiang, B. Li and Y. Wang, *Image Processing Method of Monitoring Information System for Meat Product Processing Tine. C.N. Patent No. CN20181114 2508.X* (2018) filed 2018-09-28.
15. H. Pu, D. W. Sun, J. Ma, D. Liu and M. Kamruzzaman, Hierarchical variable selection for predicting chemical constituents in lamb meats using hyperspectral imaging, *J. Food Eng.* **143** (2014) 44–52.
16. V. S. Kodogiannis, E. Kontogianni and J. N. Lygouras, Neural network based identification of meat spoilage using Fourier-transform infrared spectra, *J. Food Eng.* **142** (2014) 118–131.
17. F. G. Del Moral, F. O'Valle, M. Masseroli and R. G. Del Moral, Image analysis application for automatic quantification of intramuscular connective tissue in meat, *J. Food Eng.* **81**(1) (2007) 33–41.
18. M. Arora, M. K. Dutta, C. M. Travieso and R. Burget, Image processing based classification of enzymatic browning in chopped apples, *2018 IEEE Int. Work Conf. Bioinspired Intelligence (IWOBI)* (2018), pp. 1–8, IEEE.
19. I. M. Nolasco-Perez, L. A. Rocco, J. P. Cruz-Tirado, M. A. Pollonio, S. Barbon, A. P. A. Barbon and D. F. Barbin, Comparison of rapid techniques for classification of ground meat, *Biosyst. Eng.* **183** (2019) 151–159.
20. F. Pena, A. Molina, C. Aviles, M. Juarez and A. Horcada, Marbling in the longissimus thoracis muscle from lean cattle breeds. Computer image analysis of fresh versus stained meat samples, *Meat Sci.* **95**(3) (2013) 512–519.
21. C. H. Trinderup, A. Dahl, K. Jensen, J. M. Carstensen and K. Conradsen, Comparison of a multispectral vision system and a colorimeter for the assessment of meat color, *Meat Sci.* **102** (2015) 1–7.
22. A. Girolami, F. Napolitano, D. Faraone and A. Braghieri, Measurement of meat color using a computer vision system, *Meat Sci.* **93**(1) (2013) 111–118.
23. G. M. Farinella, D. Allegra, M. Moltisanti, F. Stanco and S. Battiato, Retrieval and classification of food images, *Comput. Biol. Med.* **77** (2016) 23–39.
24. J. H. Cheng and D. W. Sun, Data fusion and hyperspectral imaging in tandem with least squares-support vector machine for prediction of sensory quality index scores of fish fillet, *LWT-Food Sci. Technol.* **63**(2) (2015) 892–898.

25. Z. Xiong, D. W. Sun, H. Pu, Z. Zhu and M. Luo, Combination of spectra and texture data of hyperspectral imaging for differentiating between free-range and broiler chicken meats, *LWT-Food Sci. Technol.* **60**(2) (2015) 649–655.
26. L. Zhou, C. Zhang, F. Liu, Z. Qiu and Y. He, Application of Deep Learning in Food: A Review. Comprehensive Reviews in Food Science and Food Safety (2019).
27. M. I. Razzak, S. Naz and A. Zaib, Deep learning for medical image processing: Overview, challenges and the future, *Classification in BioApps* (Springer, Cham, 2018), pp. 323–350.
28. A. Maier, C. Syben, T. Lasser and C. Riess, A gentle introduction to deep learning in medical image processing, *Zeitschriftfür Medizinische Physik* **29**(2) (2019) 86–101.
29. S. B. Fatemi and S. Gholinejad, Assessing the effectiveness of Google Earth images for spatial enhancement of RapidEye multi-spectral imagery, *Int. J. Remote Sens.* **40**(12) (2019) 4526-4543.
30. F. Xing, Y. Xie, H. Su, F. Liu and L. Yang, Deep learning in microscopy image analysis: A survey, *IEEE Trans. Neural Netw. Learn. Syst.* **29**(10) (2017) 4550–4568.
31. A. Kamilaris and F. X. Prenafeta-Boldú, Deep learning in agriculture: A survey, *Comput. Electron. Agriculture* **147** (2018) 70–90.
32. D. Han, Q. Liu and W. Fan, A new image classification method using CNN transfer learning and web data augmentation, *Expert Syst. Appl.* **95** (2018) 43–56.
33. A. Krizhevsky, I. Sutskever and G. E. Hinton, Imagenet classification with deep convolutional neural networks, *Adv. Neural Inform. Process. Syst.* (2012) 1097–1105.
34. H. W. Ng, V. D. Nguyen, V. Vonikakis and S. Winkler, Deep learning for emotion recognition on small datasets using transfer learning, *Proc. 2015 ACM on Int. Conf. Multimodal Interaction* (2015), pp. 443–449, ACM.
35. M. Al-Sarayreh, M. Reis, W. Qi Yan and R. Klette, Detection of red-meat adulteration by deep spectral–spatial features in hyperspectral images, *J. Imag.* **4**(5) (2018) 63.
36. Y. Kawano and K. Yanai, Automatic expansion of a food image dataset leveraging existing categories with domain adaptation, *European Conf. Computer Vision* (Springer, Cham, 2014), pp. 3–17.
37. J. Deng, W. Dong, R. Socher, L. J. Li, K. Li and L. Fei-Fei, Imagenet: A large-scale hierarchical image database, *2009 IEEE Conf. Computer Vision and Pattern Recognition*, 2009, pp. 248–255, IEEE.
38. F. Feigl and C. C. Neto, Spot Tests for Detection of N-Nitroso Compounds (Nitrosamines), *Anal. Chem.* **28**(8) (1956) 1311–1312.
39. M. Mittal, R. K. Sharma and V. P. Singh, Performance evaluation of threshold-based and k-means clustering algorithms using iris dataset, *Recent Patents Eng.* **13**(2) (2019) 131–135.
40. M. M. Galloway, Texture analysis using grey level run lengths, *STIN* **75** (1974) 18555.
41. A. Chu, C. M. Sehgal and J. F. Greenleaf, Use of gray value distribution of run lengths for texture analysis, *Pattern Recog. Lett.* **11**(6) (1990) 415–419.
42. B. V. Dasarathy and E. B. Holder, Image characterizations based on joint gray level—run length distributions, *Pattern Recogn. Lett.* **12**(8) (1991) 497–502.
43. B. Ravikumar, D. Thukaram and H. P. Khincha, Comparison of multiclass SVM classification methods to use in a supportive system for distance relay coordination, *IEEE Trans. Power Delivery* **25**(3) (2010) 1296–1305.
44. S. Doraisamy, S. Golzari, N. Mohd, M. N. Sulaiman and N. I. Udzir, A study on feature selection and classification techniques for automatic genre classification of traditional Malay music. In *ISMIR* (2008), pp. 331–336.
45. A. Arauzo-Azofra, J. L. Aznarte and J. M. Benítez, Empirical study of feature selection methods based on individual feature evaluation for classification problems, *Expert Syst. Appl.* **38**(7) (2011) 8170–8177.

46. A. Payal, C. S. Rai and B. R. Reddy, Analysis of some feedforward artificial neural network training algorithms for developing localization framework in wireless sensor networks, *Wireless Personal Commun.* **82**(4) (2015) 2519–2536.
47. K. He, X. Zhang, S. Ren and J. Sun, Deep residual learning for image recognition, In *Proc. IEEE Conf. Computer Vision and Pattern Recognition* (2016), pp. 770–778.
48. K. Simonyan and A. Zisserman, Very deep convolutional networks for large-scale image recognition, arXiv preprint arXiv: (2014) 1409.1556.
49. O. Russakovsky, J. Deng, H. Su, J. Krause, S. Satheesh, S. Ma and A. C. Berg, Imagenet large scale visual recognition challenge, *Int. J. Comput. Vis.* **115**(3) (2015) 211–252.
50. A. G. Howard, M. Zhu, B. Chen, D. Kalenichenko, W. Wang, T. Weyand, M. Andreetto and H. Adam, Mobilenets: Efficient convolutional neural networks for mobile vision applications, arXiv preprint arXiv:1704.04861 (2017).
51. H. C. Shin, H. R. Roth, M. Gao, L. Lu, Z. Xu, I. Nogues, J. Yao, D. Mollura and R. M. Summers, Deep convolutional neural networks for computer-aided detection: CNN architectures, dataset characteristics and transfer learning, *IEEE Trans. Med. Imaging* **35**(5) (2016) 1285–1298.
52. Y. Bar, I. Diamant, L. Wolf, S. Lieberman, E. Konen and H. Greenspan, Chest pathology detection using deep learning with non–medical training, in *2015 IEEE 12th Int. Symp. Biomedical Imaging (ISBI)* (2015), pp. 294–297, IEEE.
53. N. Tajbakhsh, J. Y. Shin, S. R. Gurudu, R. T. Hurst, C. B. Kendall, M. B. Gotway and J. Liang, Convolutional neural networks for medical image analysis: Full training or fine tuning? *IEEE Trans. Med. Imaging* **35**(5) (2016) 1299–1312.
54. J. Howard and S. Gugger, Fastai: A layered API for deep learning, *Information* **11**(2) (2020) 108.
55. H. Li, Q. Chen, J. Zhao and M. Wu, Nondestructive detection of total volatile basic nitrogen (TVB-N) content in pork meat by integrating hyperspectral imaging and colorimetric sensor combined with a nonlinear data fusion, *LWT-Food Sci. Technol.* **63**(1) (2015) 268–274.
56. W. Cheng, D. W. Sun, H. Pu and Y. Liu, Integration of spectral and textural data for enhancing hyperspectral prediction of K value in pork meat, *LWT-Food Sci. Technol.* **72** (2016) 322–329.
57. M. Al-Sarayreh, M. M. Reis, W. Q. Yan and R. Klette, Detection of adulteration in red meat species using hyperspectral imaging, *Pacific-Rim Symp. Image and Video Technology* (2017), pp. 182–196, Springer, Cham.
58. X. Sun, J. Young, J. H. Liu and D. Newman, Prediction of pork loin quality using online computer vision system and artificial intelligence model, *Meat Sci.* **140** (2018) 72–77.
59. X. Yu, J. Wang, S. Wen, J. Yang and F. Zhang, A deep learning based feature extraction method on hyperspectral images for nondestructive prediction of TVB-N content in Pacific white shrimp (Litopenaeusvannamei), *Biosyst. Eng.* **178** (2019) 244–255.